

# Reduction of Ethanol Yield from Switchgrass Infected with Rust Caused by *Puccinia emaculata*

Virginia R. Sykes<sup>1</sup> · Fred L. Allen<sup>1</sup> · Jonathan R. Mielenz<sup>2,5</sup> · C. Neal Stewart Jr.<sup>1,2</sup> · Mark T. Windham<sup>3</sup> · Choo Y. Hamilton<sup>2,6</sup> · Miguel Rodriguez Jr.<sup>2,4</sup> · Kelsey L. Yee<sup>2,7</sup>

© Springer Science+Business Media New York 2015

**Abstract** Switchgrass (*Panicum virgatum*) is an important biofuel crop candidate thought to have low disease susceptibility. As switchgrass production becomes more prevalent, monoculture and production fields in close proximity to one another may increase the spread and severity of diseases such as switchgrass rust caused by the pathogen *Puccinia emaculata*. The objective of this research was to examine the impact of rust on ethanol yield in switchgrass. In 2010 and 2012, naturally infected leaves from field-grown ‘Alamo’ and ‘Kanlow’ in Knoxville, TN (2010, 2012) and Crossville, TN (2012) were visually categorized as exhibiting low, medium, or high disease based on the degree of chlorosis and sporulation. *P. emaculata* was isolated from each disease range to confirm infection. Samples from 2010 were acid/heat pretreated and subjected to two runs of simultaneous saccharification and fermentation

(SSF) with *Saccharomyces cerevisiae* D<sub>5</sub>A to measure ethanol yield. Near-infrared spectroscopy (NIRS) was used to estimate ethanol yield for 2012 samples. SSF and NIRS data were analyzed separately using ANOVA. Disease level effects were significant within both models ( $P < 0.05$ ) and both models explained a large amount of variation in ETOH (SSF:  $R^2 = 0.99$ , NIRS:  $R^2 = 0.99$ ). In the SSF dataset, ethanol was reduced by 35 % in samples exhibiting medium disease symptoms and by 55 % in samples exhibiting high disease symptoms. In the NIRS dataset, estimated ethanol was reduced by 10 % in samples exhibiting medium disease symptoms and by 21 % in samples exhibiting high disease symptoms. Results indicate that switchgrass rust will likely have a negative impact on ethanol yield in switchgrass grown as a biofuel crop.

**Keywords** NIRS · Rust · *Puccinia emaculata* · Switchgrass · Ethanol · SSF · *Panicum virgatum*

✉ Virginia R. Sykes  
vsykes@utk.edu

<sup>1</sup> Department of Plant Sciences, University of Tennessee, 252 Ellington Plant Sciences, 2431 Joe Johnson Drive, Knoxville, TN 37996, USA

<sup>2</sup> Bioenergy Science Center, Oak Ridge National Laboratory, Oak Ridge, TN 37831, USA

<sup>3</sup> Department of Entomology and Plant Pathology, University of Tennessee, 2505 E.J. Chapman Drive, 370 Plant Biotechnology Building, Knoxville, TN 37996, USA

<sup>4</sup> Bioconversion Science & Technology BioSciences Division, Oak Ridge National Laboratory, Oak Ridge, TN 37831, USA

<sup>5</sup> Present address: White Cliff Biosystems, Rockwood, TN 37854, USA

<sup>6</sup> Present address: Center for Renewable Carbon, 2506 Jacob Drive, Knoxville, TN 37996, USA

<sup>7</sup> Present address: Genomatica Inc., 4757 Nexus Center Drive, San Diego, CA 92121, USA

## Introduction

Switchgrass is a high yielding, perennial grass, native to North America that has received increased interest for its potential as a bioenergy crop. Switchgrass was chosen as a model herbaceous energy crop, in part, for its production ability under management systems with limited inputs [1]. While few reports of switchgrass diseases exist prior to the advent of its use as a biofuel crop, concern over potentially significant disease problems resulting from increased hectareage and production in monoculture has led to further examination of switchgrass disease susceptibility and the impact of that susceptibility on biomass yield and ethanol yield.

Over 42 fungal species have been identified as occurring on switchgrass [2]. However, most reports of switchgrass diseases are reports of incidence alone with limited information

on economic impact. Rust is one of the most frequently cited switchgrass diseases in terms of prevalence. A number of causal agents have been identified for switchgrass rust including *Puccinia emaculata* Schwein [2–6], *Puccinia virgata* Ellis & Everh., *Puccinia graminis* Pers: Pers [6–9], and *Uromyces graminicola* Burrill [4]. The probable motility of pathogens associated with switchgrass rust as switchgrass production increases and the high damage observed from rusts associated with other important agronomic crops make switchgrass rust a potential economic concern for switchgrass production.

While a pathogenic relationship between *P. emaculata* and switchgrass clearly exists, the impact of this pathogen on switchgrass yield is still somewhat unclear. Weak, but significant, negative correlations between disease and biomass yield have been reported by Hopkins et al. [5] in observations of 23 switchgrass accessions in NE, IA, and IN ( $r=-0.12$ ,  $P<0.05$ ) and by Sykes (unpublished) in observations of a lowland half-sib population in TN ( $r=-0.15$ ,  $P<0.05$ ). In both studies, while rust was the predominant disease observed, other diseases were also present in disease ratings. Hagan and Akridge [10] also noted a significant decrease in biomass from rust-infected ornamental switchgrass compared to ornamental switchgrass treated with a fungicide. This type of yield reduction has not been examined on agronomic switchgrass which may be associated with less virulent strains of *P. emaculata* compared to ornamental switchgrass varieties [11].

While these studies examine the relationship between switchgrass rust and biomass yield, they do not examine the impact of these infections on ethanol yield. As a biofuel crop, two components contribute to total biofuel yield: biomass yield and the ethanol production potential of that biomass. In addition to potentially reducing biomass yield, the potential reduction in the quality of that biomass and the resulting reduction in ethanol production may lead to a substantial loss in total biofuel yield. Further examination of the interaction of pathogen infection on the ethanol production potential of switchgrass is essential to understanding the potential threat switchgrass diseases pose to switchgrass production systems. The objective of this research was to examine the impact of switchgrass rust on ethanol yield from switchgrass.

## Materials and Methods

### Plant Material

On 27 August 2010, switchgrass leaves, ranging in level of rust severity, were collected from ten plants of ‘Alamo’ and ten plants of ‘Kanlow’. Alamo is a cultivar collected in Texas in 1977 and Kanlow is a cultivar developed in Kansas and released in 1963 (USDA National Plant Germplasm System). These two cultivars are the most commonly grown cultivars in the state of TN, with Alamo being the predominant of the two

[12]. Because switchgrass is an obligate outcrosser, both cultivars are genetically very diverse. Sampled plants were unique genotypes randomly selected from within each cultivar. Plants were in their second year of production and were grown on 1-m centers in a selection nursery at the Holston Unit of the University of Tennessee, East Tennessee Research and Education Center in Knoxville, TN (35° 58' 11.3" N, 83° 51' 08.7" W, soil type: Shady-Whitewell complex). Leaf samples were cut at the junction of the leaf and stem and did not include the leaf sheath. Composite sampling was used to account for genetic diversity among plants while reducing the overall sample size due to high laboratory analytical costs. Leaves collected in 2010 were combined into six composite samples, three per cultivar, based on visual assessment of rust severity as high disease, medium disease, or low disease. Leaves exhibiting no sporulation and little to no visible chlorosis were classified as low disease (Fig. 1a, b). Leaves exhibiting light to medium sporulation and heavy chlorosis were classified as medium disease (Fig. 1c, d). Leaves exhibiting heavy sporulation were classified as high disease (Fig. 1e, f). Leaves with symptoms indicative of infection by other pathogens were excluded. Approximately 100 leaves were collected from each disease level within each cultivar. Due to differences in rust susceptibility, not all genotypes were equally represented in each disease composite. Within each disease category, approximately four genotypes had lower numbers of leaves available that fit that disease category. Approximately equal numbers of leaves were collected from the remaining genotypes. While collecting an equal number of leaves from each genotype would have been preferable, the use of composite sampling from within two genetically diverse cultivars and from multiple locations was done to help alleviate the potential influence of genetic differences in ethanol yield on results. Plants were all in the reproductive-floral development stage of growth at the time of collection [13]. Low disease leaves were often only available from tillers in the late E stages, while medium and high disease leaves were collected from tillers in the R4 and R5 stages. To account for these differences in developmental stage, healthy leaves from a disease-free greenhouse-grown clone of Alamo were collected from tillers in the late E stages and from tillers in the R4 to R5 stages to serve as controls.

Sample collection was repeated on 1 August 2012 with samples collected again from the selection nursery in Knoxville, TN and also from swards of Alamo and Kanlow grown in Crossville, TN (36° 00' 49.7", N 85° 07' 57.7" W, soil type: Lonewood loam). In 2012, composite samples by disease level (high, medium, low) were created for each cultivar (Alamo, Kanlow) at each location (Knoxville, Crossville), resulting in a total of 12 samples. After collection, leaves were placed in mesh bags and dried in an oven at 45 °C for 48 h. Dried leaves were then ground to pass through a 1-mm mesh using a Cyclone sample mill (UDY Corp., Fort Collins, CO).

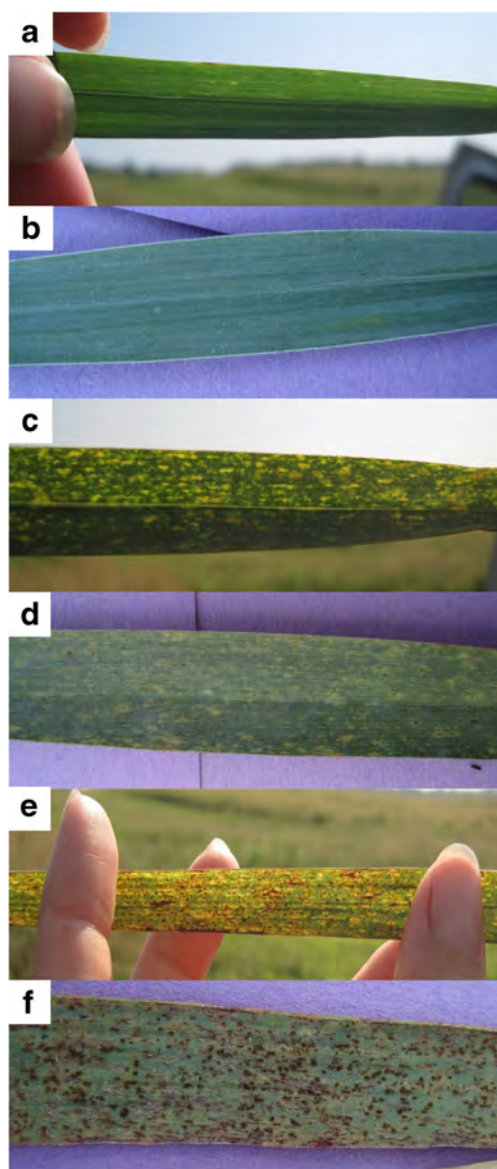


**Fig. 1** Switchgrass leaves, viewed under two light conditions (backlighting: **a**, **c**, **e**; incident lighting: **b**, **d**, **f**), expressing low disease symptoms—no sporulation and little to no chlorosis (**a**, **b**), medium disease symptoms—light to medium sporulation and medium chlorosis (**c**, **d**), and high disease symptoms—heavy sporulation and chlorosis (**e**, **f**)

### Pathogen Isolation and Identification

Prior to drying, *P. emaculata* was isolated from a sample of leaves within each disease stage to satisfy Koch's postulates and confirm infection. The pathogen was isolated by touching a sterile scalpel blade to a single pustule on an infected leaf and then touching the scalpel blade to a drop of distilled water on a detached leaf segment of Alamo switchgrass. Cultures were maintained on fresh Alamo leaves placed on moistened filter paper within a petri dish sealed with parafilm. Naturally infected leaves and cultured isolates were refrigerated for several weeks to induce production of teliospores (Yonghao Li,

personal communication). Naturally infected leaves and cultured isolates were examined, and images were captured using a Nikon Eclipse 80i microscope (Nikon Instruments Inc., Melville, NY) with attached Digital Sight DS-2MV camera (Nikon Instruments Inc., Melville, NY) to characterize the morphologies of urediniospores and a Motic BA400 compound microscope (Motic North America, Richmond, British Columbia, Canada) with attached Canon EOS Rebel XTi camera (Canon U.S.A., Inc., Melville, NY) to characterize the morphologies of teliospores.

### Ethanol Fermentation

Dried, ground biomass collected in 2010 was subjected to ethanol fermentation using simultaneous saccharification and fermentation (SSF) as described by Dowe and McMillan [14] preceded by chemical and thermal pretreatment as described by Fu et al. [15].

To pretreat material, 72 ml of 0.5 %  $H_2SO_4$  was added to 8 g of dried, ground biomass in a Pyrex bottle and allowed to stand at room temperature overnight (~18 h). The solution was then centrifuged at  $10,967\times g$  for 20 min in a 50-ml disposable centrifuge tube in a Sorvall Legend XTR (Thermo Scientific) centrifuge. The supernatant was discarded and the remaining biomass solid was divided into two metal reactors, each holding approximately 2.5 g on a dry basis. Reactors were heated in boiling water for 2 min, placed in a sand bath set at 160 °C for 7 min, and then quenched in an ice bath for 2 min. Twenty-five milliliters of Milli-Q water was added to the biomass from each reactor and agitated to suspend. Samples were then centrifuged at  $10,968\times g$  for 20 min. The supernatant was retained and the cellulose content of the material after pretreatment was determined by quantitative saccharification using high-performance liquid chromatography (HPLC) method ASTM E 1758-01 (ASTM 2003) and HPLC method NREL/TP 51-42623 on a HPLC LaChrom Elite® system (Hitachi High Technologies America, Inc.). Each biomass sample was then washed three consecutive times with 225 ml of Milli-Q water using vacuum filtration between each wash. To determine dry basis weights, samples of 0.5 g of washed biomass were weighed out in triplicate from each treatment and dried in an oven until the dry weight remained constant (approximately 24 to 48 h). The remaining washed biomass was placed in a 50-ml tube and stored along with washate samples in a -20 °C freezer.

Pretreatment was followed by SSF with *Saccharomyces cerevisiae* D<sub>5</sub>A. Protocol and all solutions, media, and stock cultures have been previously described by Dowe and McMillan [14]. Ethanol fermentations contained three technical replications per treatment. Sealed 70-ml reusable BBL Septi-Chek bottles were each loaded with 0.4 g of biomass on a dry basis and 15 ml of deionized water. Bottles were then autoclaved for 30 min on a liquid cycle. *S. cerevisiae* D<sub>5</sub>A,

originating from a single colony grown on a yeast extract peptone dextrose (YPD) plate incubated at 35 °C for 24–48 h, was increased in YPD broth agitated at 150 rpm for 24 h at 35 °C. Upon cooling, Spezyme CP at a loading of 15 filter paper units (FPU) g cellulose<sup>-1</sup>, Accelerase BG at a 25 % volume ratio to Spezyme, 0.5 ml of the yeast cell inoculum, 1 ml of 10× YP solution, 1 ml of 1-M citrate buffer, 50 µl of a 25 µg ml<sup>-1</sup> streptomycin solution, and water in amounts required to achieve a final solution weight of 20 g were added to each bottle. Enzymes were provided by Genencor International. Bottles were sealed, weighed to the nearest 1000th of a gram, and placed in a New Brunswick C24 shaker (New Brunswick Instrument Company, New Brunswick, NJ) at 36 °C and 150 rpm. At 14, 24, 36, 60, 132, 204, and 300 h after inoculation, bottles were vented with a sterile needle to release CO<sub>2</sub> and then the bottles were weighed. Bottle weight loss was used as an indicator of fermentation rate. After the final weighing period, samples were centrifuged at 13,000 rpm for 20 min, and the supernatant was filtered through a 0.22-µm syringe tip filter (Fisher Scientific, Atlanta, GA). A HPLC LaChrom Elite<sup>®</sup> system (Hitachi High Technologies America, Inc.) equipped with a refractive index detector (model L-2490) was used to measure ethanol concentrations (mg g<sup>-1</sup>) in culture filtrates using an Aminex<sup>®</sup> HPX-87H column (Bio-Rad Laboratories, Inc.) at a flow rate of 0.5 ml/min of 5.0-mM sulfuric acid and a column temperature of 60 °C.

### Near-Infrared Reflectance Spectroscopy Analysis

Because of the time and expense of the SSF procedures described above, 2012 samples were analyzed using near-infrared reflectance spectroscopy (NIRS) to estimate ethanol yield. Samples were analyzed using a FOSS NIRSystems 4500 Feed & Forage Analyzer (FOSS Analytical, Hillerød, Denmark). WINISI II software, supplied by Infrasoftware International LLC (State College, PA), was used for NIRS analysis. The WINISI II software includes appropriate files to report Global H (GH) values for all analytes. Values greater than 3 indicate that the analyte may be an outlier when compared to the dataset from which the calibration equation was developed [16]. Although Vogel et al. [17] developed NIRS calibrations specifically for estimating ethanol production from switchgrass, the samples from this rust severity experiment were not within the spectral profile of the calibration set for estimating ethanol yield, possibly due to the diseased nature of the material. All samples did fit the 2013 mixed hay equation (GH < 3) published by the NIRS Consortium [18]. Using this equation, values were estimated for neutral detergent fiber (NDF) and digestible neutral detergent fiber from an in vitro neutral detergent fiber digestion for 48 h (dNDF48). These values were then inserted into a regression equation that Lorenz et al. [19] developed to estimate SSF-derived ethanol yield from corn stover. Since the published regression

equation was developed for corn stover and not switchgrass, 2010 switchgrass samples, on which SSF had been performed, were used to validate the regression equation by examining the correlation between ethanol values derived from SSF and ethanol values predicted using NIRS. The fit was further examined by comparing the square root of the mean square error (MSE) from the original corn stover data to the square root of the MSE of the 2010 switchgrass SSF data fitted to the predicted ethanol regression equation.

Using NIRS and the 2013 mixed hay equation [18], additional compositional element values were estimated for the combined 2010 and 2012 sample set. These components include protein, acid detergent fiber (ADF), NDF, lignin, ash, dNDF48, neutral detergent fiber digestibility at 48 h (NDFD48), sugars, fructan, magnesium, and calcium. Percent cellulose was calculated as ADF minus lignin. Percent hemicellulose was calculated as NDF minus ADF.

### Statistical Analysis

Data were analyzed separately by year since different analytical methods were used to assess ethanol yield in 2010 (SSF) compared to 2012 (NIRS) and because 2012 data contained a location effect. Within each year, a mixed model ANOVA ( $\alpha=0.05$ ) was run in SAS (v. 9.3, Cary, NC). In the SSF ANOVA model, the error term represents technical replication of each experimental unit. The NIRS ANOVA model was designed as a split-plot, replicated by location, and did not contain technical replication. In the NIRS ANOVA model, location and cultivar\*location were considered random. The SSF and NIRS ANOVA models are described below:

$$\text{SSF} : Y_{ijk} = \mu + \text{disease}_i + \text{cultivar}_j \\ + \text{disease} * \text{cultivar}_{ij} + \text{error}_{ijk}$$

where  $Y_{ijk}$  is the ethanol yield in the experimental unit from the  $i$ th disease level,  $j$ th cultivar, and  $k$ th run; mean ethanol yield is  $\mu$ ;  $\text{disease}_i$  is the effect of the  $i$ th disease level (high, medium, or low);  $\text{cultivar}_j$  is the effect of the  $j$ th cultivar (Alamo, Kanlow);  $\text{disease} * \text{cultivar}_{ij}$  is the interaction effect of the  $i$ th disease level and  $j$ th cultivar; and  $\text{error}_{ijk}$  is the experimental error from the  $i$ th disease level,  $j$ th cultivar, and  $k$ th technical replication. An additional model, including just a treatment and error effect, was used to examine differences between ethanol yield from biomass collected from R3 to R4 stage tillers and V stage tillers of the greenhouse-grown Alamo control.

$$\text{NIRS} : Y_{ijk} = \mu + \text{disease}_i + \text{cultivar}_j + \text{location}_k \\ + \text{disease} * \text{cultivar}_{ij} + \text{disease} * \text{location}_{ik} \\ + \text{cultivar} * \text{location}_{jk} + \text{error}_{ijk}$$

where all effects are as described above with the exception to additions of the location effect, location interaction effects, and the error terms, which include the cultivar\*location effect which accounts for the error term for the main plot, cultivar, in the split-plot design, and the error term for the subplot which represents the  $i$ th disease level,  $j$ th cultivar, and  $k$ th location. Means within significant effects were separated using Student's  $t$  test for tests of two means and Tukey's honestly significant difference (HSD) method for tests of three means using options within the MIXED procedure in SAS [20].

NIRS was performed on samples from both years, and this combined dataset was used to assess the relationship between disease and various compositional elements. NIRS data for compositional elements were analyzed using an ANOVA ( $\alpha=0.05$ ) in SAS with disease level as the independent variable and each compositional element as the dependent variable within respective models. Within significant models, means were separated using Tukey's HSD.

## Results and Discussion

*P. emaculata* was successfully isolated from the leaves classified as medium and high disease severity but not from the leaves classified as low disease severity. Symptoms and signs were observed on both leaves collected from the field and on inoculated leaves. Symptoms and signs presented as yellow flecking that progressed into orange pustules containing urediniospores erupting through the epidermis (Fig. 2a). In plants exhibiting medium to heavy sporulation, early senescence was also observed. Urediniospores were cinnamon brown, broadly ellipsoid, and, on average, 23  $\mu\text{m}$  in diameter ( $n=20$ ,  $s=1.7$ ; Fig. 2b). Teliospores were chestnut brown, rounded above, and narrowed below with a slight constriction at the septum and a brown pedicel approximately one times the length of the spore (Fig. 2c). Measurements were not taken of teliospore diameters due to equipment availability. The pathogen causing rust disease symptoms was identified as *P. emaculata* based on host plant and morphology of urediniospores and teliospores as described by Arthur [21].

Estimates of ethanol yield from 2010 switchgrass samples using NIRS and the equation developed by Lorenz et al. [19] for corn stover were compared to the average ethanol yield from the SSF replications of 2010 switchgrass samples to determine whether this equation was appropriate for estimating ethanol yield of the 2012 sample set. The resulting Pearson correlation was significant ( $P=0.008$ ) and showed a high correlation of NIRS-predicted ethanol yield to SSF ethanol yield ( $R=0.97$ ). A Spearman correlation was also calculated and indicated a very strong association between ranking of NIRS-predicted ethanol yield and SSF ethanol yield ( $R=1$ ). The square root of the MSE was calculated to further examine the goodness of fit. The square root of the MSE for the original

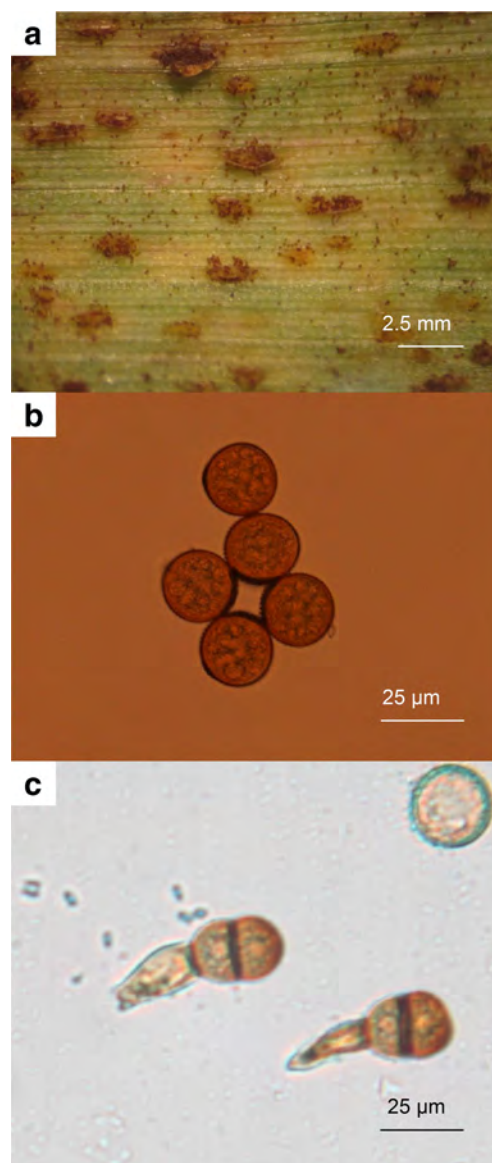


**Fig. 2** Magnification of pustules erupting through switchgrass epidermis (a) and micrographs of urediniospores (b) and teliospores (c) from cultures isolated from field-grown switchgrass naturally infected with *Puccinia emaculata*

corn stover data was 1.8  $\text{mg g}^{-1}$ , while the square root of the MSE for the 2010 SSF data was 9.7  $\text{mg g}^{-1}$ . The higher value observed in the SSF data is likely due to the fact that the original corn stover regression equation was developed without examining a holdout sample, which tends to result in a regression equation that is overfit to the data. Additionally, the corn stover data did not contain the lower range of ethanol values observed in the 2010 SSF data. While the equation did an excellent job of predicting ethanol yield from medium disease samples, it did tend to overestimate ethanol yield of samples exhibiting low ethanol yield and slightly underestimate ethanol yield from samples exhibiting high ethanol yield (Fig. 3). Although this equation does not give an exact

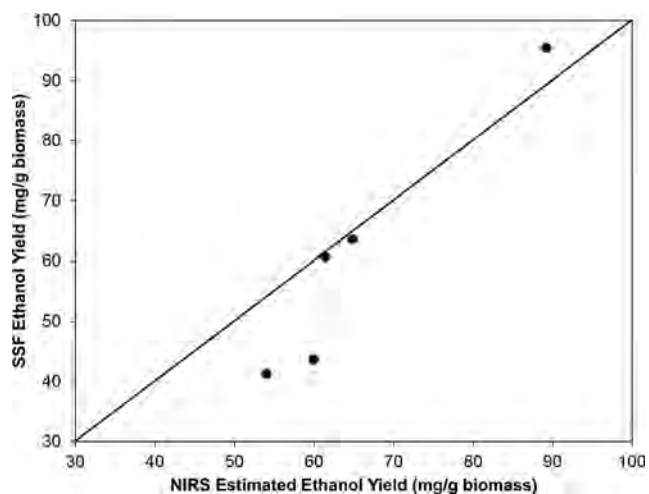
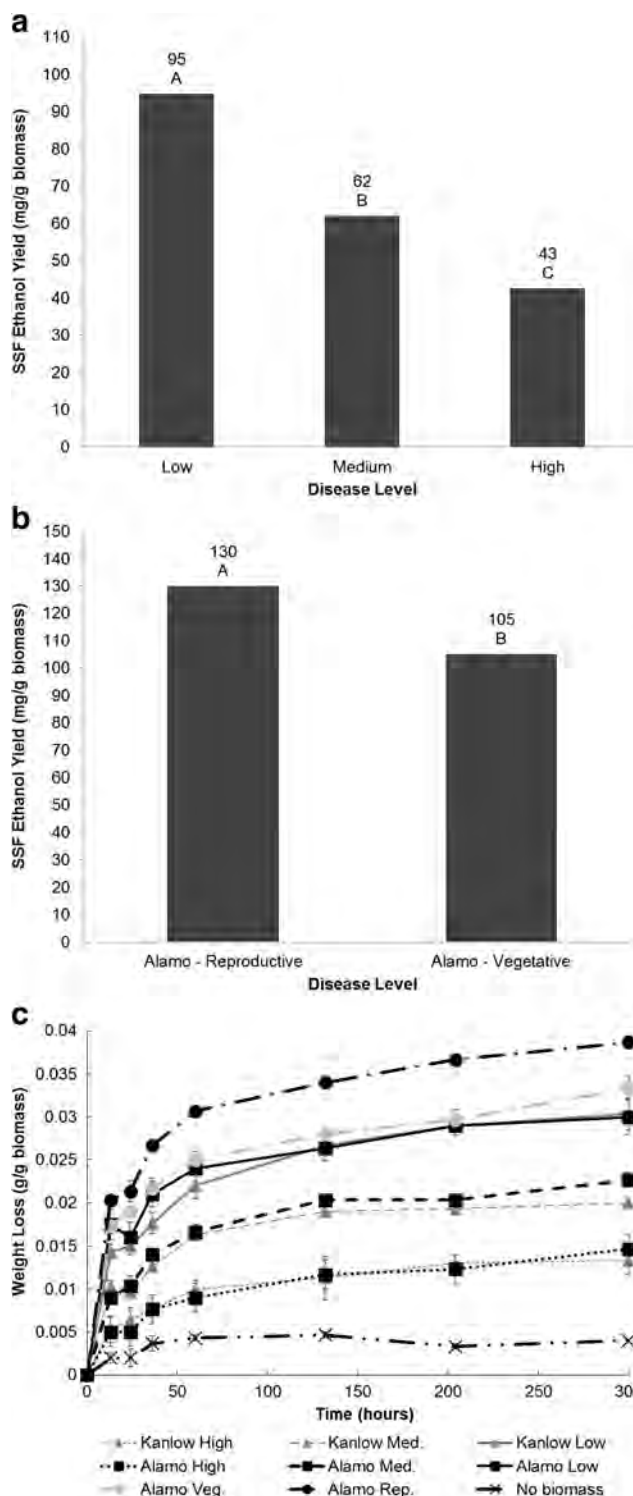


**Fig. 3** Plot of SSF ethanol yields (y axis) from 2010 samples against ethanol yields predicted using the regression equation developed by Lorenz with NDF and dNDF48 values estimated using near-infrared spectroscopy (NIRS) (x axis). The solid line represents a perfect fit with a slope of 1 and an intercept of 0. Deviations from this line indicate differences in actual (SSF) and predicted (NIRS) ethanol yield values

measurement of ethanol yield from switchgrass, it does provide a good estimate of ethanol yield and an excellent prediction of ranking.

The 2010 model (SSF) explained a large portion of the variation in ethanol yield ( $R^2=0.99$ ), and disease level was a significant effect ( $P<0.001$ ) within the model. Cultivar was not significant and there was no significant interaction between cultivar and disease. The average ethanol yield from medium disease samples ( $62 \text{ mg g}^{-1}$  biomass) and high disease samples ( $43 \text{ mg g}^{-1}$  biomass) was significantly lower than the ethanol yield from low disease samples ( $95 \text{ mg g}^{-1}$  biomass; Fig. 4a). Compared to the ethanol yield from low disease samples, medium disease samples had a 35 % reduction in ethanol yield and high disease samples had a 55 % reduction in ethanol yield. Fermentation rates were monitored using change in bottle weights due to  $\text{CO}_2$  release. A clear distinction in fermentation rate can be observed between high, medium, and low disease samples, with samples exhibiting medium and high disease severity showing slower fermentation rates compared to samples exhibiting low disease severity (Fig. 4c).

Ethanol yield differed significantly between the leaves collected from tillers in reproductive growth stages and the leaves collected from tillers in vegetative growth stages from greenhouse-grown Alamo clones. The leaves collected from tillers in the reproductive stage produced significantly more ethanol than the leaves collected from tillers in the vegetative stage (Fig. 4b). Since low disease leaves, which were primarily collected from tillers in the vegetative growth stage, had higher ethanol yield than medium and high disease leaves, which were collected from tillers in the reproductive growth stages, results indicate that the reduction in ethanol yield from



the leaves with medium and high levels of rust severity may be even greater than what was observed in this experiment. These results are not consistent with other studies that show a decrease in digestibility due to increases in NDF and lignin and decreases in cellulose as switchgrass reaches physiological maturity [22]. However, Jung and Vogel [22] did note that the magnitude of these changes was much smaller in the

◀ **Fig. 4** Ethanol yield ( $\text{mg g}^{-1}$  biomass) as determined by simultaneous saccharification and fermentation (SSF) of switchgrass leaves collected from Knoxville, TN in 2010. Means followed by the same letter do not differ significantly at  $\alpha=0.05$ . **a** Ethanol yields from disease treatments averaged across cultivar since no significant interactions with disease were observed. **b** Ethanol yields from the leaves collected from tillers in the reproductive (R4–R5) or vegetative (V) growth stage from a greenhouse-grown Alamo clone. **c** Weight loss of fermentation bottles due to  $\text{CO}_2$  release over time for Alamo and Kanlow cultivars at each level of disease severity (low, medium, high) and for reproductive and vegetative growth stage Alamo controls. Data points represent the weight loss throughout the SSF run  $\pm$  SE of the three technical replications

leaves compared to the stems. Additionally, these previous studies examined differences between plants that were in different growth stages, whereas in this experiment, the switchgrass plants were all in the R4–R5 stages of growth with leaves collected from individual tillers on that plant that were either in the vegetative or reproductive growth stage.

The 2012 model (NIRS) also explained a large portion of variation in ethanol yield ( $R^2=0.99$ ), and disease level was again a significant effect ( $P=0.009$ ) within the model. Cultivar was significant, with Kanlow producing higher ethanol yields ( $72 \text{ mg g}^{-1}$  biomass) compared to Alamo ( $70 \text{ mg g}^{-1}$  biomass); however, location was not significant and neither cultivar nor location showed a significant interaction with disease. The estimated mean ethanol yield from medium disease samples ( $72 \text{ mg g}^{-1}$  biomass) and high disease samples ( $63 \text{ mg g}^{-1}$  biomass) was significantly lower than the estimated ethanol yield from low disease samples ( $80 \text{ mg g}^{-1}$  biomass; Fig. 5). Compared to the estimated ethanol yield from low disease samples, medium disease samples had a

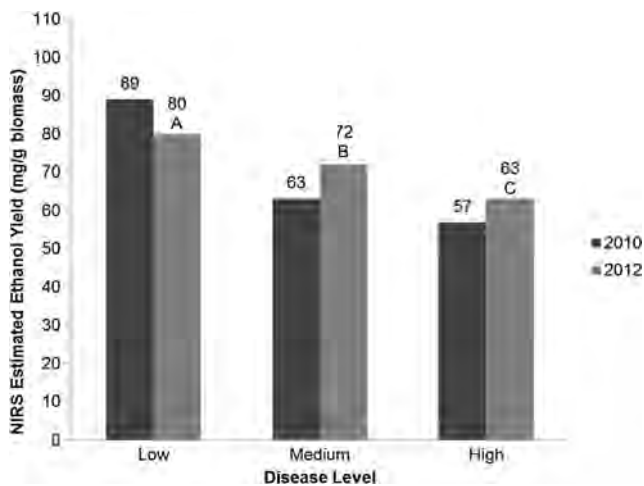


**Fig. 5** Ethanol yield ( $\text{mg g}^{-1}$ ) as estimated using near-infrared spectroscopy (NIRS) of switchgrass leaves collected from Knoxville, TN in 2010 and Knoxville, TN and Crossville, TN in 2012. Estimated ethanol yields were averaged across cultivar and location since no significant interactions with disease were observed. Means followed by the same letter do not differ significantly at  $\alpha=0.05$ . Mean separation was not performed on 2010 samples due to a shortage of material available for NIRS analysis resulting in only a single data point for the low disease category

10 % reduction in estimated ethanol yield, and high disease samples had a 21 % reduction in estimated ethanol yield. Estimates using NIRS of 2010 samples are also given in Fig. 4. Because all of the Alamo low disease material was used in the SSF procedure and was not available for NIRS analysis, leaving only a single 2010 NIRS low disease data point, mean separation was not performed on NIRS 2010 data. However, means are given for comparison to 2012 NIRS results. Disease in 2010 appears to have caused a greater reduction in ethanol yield compared to 2012. This may have been due to the fact that 2010 samples were collected in the latter part of August, compared to 2012 samples which were collected at the beginning of August, allowing more time for the rust pathogen to infect. The same trend is seen in both years, though, with a clear reduction in ethanol yield as disease severity increases. Results from the NIRS data show a less drastic decrease in ethanol yield compared to yield reductions observed from SSF data. The difference in estimated ethanol yield reduction between the SSF and NIRS models is likely due to the NIRS prediction equation, which tended to draw ethanol yield values from the top and bottom yielding samples toward more median values. Results from the SSF model are likely more indicative of actual ethanol yield losses due to disease; however, results from the NIRS model collaborate results from the SSF model in terms of ranking.

Compositional elements that differed significantly by disease level included dry matter ( $P=0.0002$ ), cellulose ( $P=0.001$ ), hemicellulose ( $P=0.018$ ), dNDF48 ( $P<0.0001$ ), NDFD48 ( $P=0.001$ ), ADF ( $P=0.001$ ), ash ( $P=0.004$ ), fat ( $P=0.008$ ), magnesium ( $P=0.0003$ ), and calcium ( $P<0.001$ ; Table 1). Models were not significant for the following dependent variables: protein, NDF, lignin, sugars, fructan, potassium, and phosphorus.

Results from this study indicate a significant reduction in ethanol yield from switchgrass infected with *P. emaculata*. Reductions in ethanol yield may be due to a number of factors shown to be associated with fungal infections. These factors can be divided into two categories: alteration of digestible plant material and reduction in digestibility of that material.

Previous studies have shown associations of rust with reduced digestibility due to an increase in fibrous, indigestible cell wall components such as cellulose and lignin. In forage, these components are measured directly or in combination through analysis of ADF, which refers to the amount of cellulose and lignin in a plant, and NDF, which refers to the amount of hemicellulose, cellulose, and lignin. Wilson et al. [23] showed that infections of *Puccinia substriata* Ellis and Barth. var. *indica* Ramachar and Cummins reduced the digestibility of pearl millet (*Pennisetum glaucum* (L.) R. Br. K. Schum.). Likewise, in studies of southern corn rust (*Puccinia polysora* Underw.) of corn (*Zea mays* L.), Queiroz et al. [24] reported an increase in NDF and a decrease of up to 16 % digestibility in corn with high rust severity, and Johnson

**Table 1** Mean component value on a percentage basis and  $R^2$  value of the ANOVA model for compositional elements estimated using near-infrared spectroscopy

Component	Mean component value by disease level (%)			$R^2$
	Low	Medium	High	
DM***	93.90a <sup>a</sup>	93.41a	92.61b	0.71
Cellulose***	30.48b	31.66b	33.46a	0.63
Hemicellulose*	27.69a	25.87ab	23.35b	0.44
dNDF48***	33.06a	29.50b	27.32c	0.78
NDFD48***	54.53a	49.28b	46.15b	0.66
ADF**	36.06a	33.07b	34.09b	0.62
Ash**	5.17b	6.36ab	7.63a	0.55
Fat*	2.18b	2.42ab	2.52a	0.48
Mg***	0.21b	0.27b	0.33a	0.68
Ca***	0.41c	0.53b	0.62a	0.87

Only elements that exhibited significant association with rust severity ( $P < 0.05$ ) are listed. Means are given for categories of low, medium, and high rust severity

\* $P < 0.05$ , \*\* $P < 0.01$ , and \*\*\* $P < 0.001$ , respectively, for the ANOVA model

<sup>a</sup> Means were separated using Tukey's HSD. Means followed by the same letter do not differ significantly ( $P < 0.05$ ) between disease levels within each compositional element, respectively

et al. [25] reported an increase in dry matter, NDF, and ADF and a decrease in dry matter digestibility in corn exhibiting rust symptoms.

We observed an increase in percent cellulose and a decrease in percent hemicellulose as disease level increased. As *Puccinia* spp. infect, they convert photosynthates to alcohols that can then be utilized by the fungus [26]. These alcohols are then used to fuel the growth of fungal structures, with the major structural components of the cell walls of *Puccinia* spp. composed of  $\beta$ -1,3-glucans and chitin [27]. The consumption of photosynthates and/or the associated increase in fungal structures may be a contributing factor to the respective decrease in percent hemicellulose and increase in percent cellulose.

The composition of digestible components may be further altered by plant defense responses to pathogen infection. Cellulose may increase during infection through encasement of the haustoria with cellulose and callose during both hypersensitive (HR) reactions in resistant genotypes and in advanced stages of rust infection in susceptible genotypes [28]. Further plant defense responses include a mechanical strengthening of cell walls. A study by Hammerschmidt [29] implicated the deposition of "stress lignin" as a potential culprit responsible for reduced digestibility in plants infected with fungal pathogens. Although "stress lignin" is well documented as a stress response which plants deploy when invaded by fungal pathogens [30–33], we did not observe any significant differences in lignin among the three rust severity levels tested.

In addition to altering the fermentable portions of the plant cell walls, pathogen infection may also increase elements that are inhibitory to the fermentation process. In our study, disease had a significant effect on percent calcium. An increase in cytoplasmic calcium has been associated with the hypersensitive response of plants to various pathogens [34, 35]. As  $\text{Ca}^{2+}$  levels increase, fermentation may be inhibited. Chotineeranat et al. [36] reported a significant inhibitory effect of  $\text{Ca}^{2+}$  on ethanol fermentation performance of *S. cerevisiae* in biofuel molasses. At concentrations of 0.72 % w/v of  $\text{Ca}^{2+}$ , ethanol yields decreased by 14–15 % compared to the control at 0 % w/v of  $\text{Ca}^{2+}$ .

## Conclusion

A very clear trend of reduced ethanol yield in switchgrass exhibiting rust symptoms was observed with reductions of 10–35 % in plants exhibiting medium disease severity and reductions of 21–55 % in plants exhibiting high disease severity. No other studies to date have examined the effect of *P. emaculata* infection on ethanol yield in switchgrass; however, these results are similar to reductions in digestibility observed in forage crops infected with *Puccinia* spp. While the exact mechanisms by which *P. emaculata* reduces ethanol yield are still speculative, the altered cell wall composition and cellular components within infected switchgrass suggest that losses may be due to a reduction in available digestible material and/or a reduction in the digestibility of that material. Results from this study suggest that biofuel production facilities may incur a hidden loss in ethanol yield when purchasing switchgrass that exhibits rust symptoms. Further studies of biomass yield loss associated with switchgrass rust, the cost and effectiveness of disease control measures, and breeding efforts to produce cultivars with reduced disease susceptibility would provide producers with more information and options for effectively managing this potentially important disease.

**Acknowledgments** We thank the funders of this research, which included the University of Tennessee AgResearch and The BioEnergy Science Center, a U.S. Department of Energy Bioenergy Research Center supported by the Office of Biological and Environmental Research in the DOE Office of Science.

## Compliance with Ethical Standards

**Conflict of Interest** The authors declare that they have no competing interests.

## References

- McLaughlin SB, Kszos LA (2005) Development of switchgrass (*Panicum virgatum*) as a bioenergy feedstock in the United States. *Biomass Bioenergy* 28(6):515–535

2. Gravert CE, Munkvold GP (2002) Fungi and diseases associated with cultivated switchgrass in Iowa. *J Iowa Acad Sci* 109(1, 2):30–34
3. Zale J, Freshour L, Agarwal S, Sorochan J, Ownley BH, Gwinn KD, Castlebury LA (2008) First report of rust on switchgrass (*Panicum virgatum*) caused by *Puccinia emaculata* in Tennessee. *Plant Dis* 92(12):1710
4. Cornelius DR, Johnston CO (1941) Differences in plant type and reaction to rust among several collections of *Panicum virgatum*. *Agron J* 33(2):115–124
5. Hopkins AA, Vogel KP, Moore KJ, Johnson KD, Carlson IT (1995) Genotypic variability and genotype × environment interactions among switchgrass accessions from the midwestern USA. *Crop Sci* 35(2):565–571
6. Cummins GB (1971) *The rust fungi of cereals, grasses, and bamboos*. Springer, New York
7. Farr DE, Bills GF, Chamuris GP, Rossman AY (1995) *Fungi on plants and plant products in the United States*. APS, St Paul
8. Tiffany LH, Knaphus G (1985) The rust fungi (*Uredinales*) of the Loess Hills region of Iowa. *J Iowa Acad Sci* 92(5):186–188
9. Gilman JC, Archer WA (1929) The fungi of Iowa parasitic on plants. *Iowa State Coll J Sci* 3:299–507
10. Hagan AK, Akridge JR (2013) Efficacy of fungicides for the control of rust on switchgrass. In: Dumenyo K (ed) *SNA Res. Conf. Pathology and Nematology*, pp 201–204
11. Li Y, Windham M, Trigiano R, Windham A, Ownley B, Gwinn K, Zale J, Spiers J (2009) Cultivar-specific interactions between switchgrass and *Puccinia emaculata*. *Phytopathology* 99(6):S72
12. Garland CD (2008) Growing and harvesting switchgrass for ethanol production in Tennessee. *UT Biofuels Initiative - SP701-A-5M-5/08*, vol SP701-A-5M-5/08. UT Extension; Knoxville, TN
13. Moore KJ, Moser LE, Vogel KP, Waller SS, Johnson BE, Pedersen JF (1991) Describing and quantifying growth stages of perennial forage grasses. *Agron J* 83(6):1073–1077
14. Dowe N, McMillan J (2001) SSF experimental protocols—lignocellulosic biomass hydrolysis and fermentation. *Laboratory Analytical Procedure*, vol NREL/TP-510-42630. National Renewable Energy Laboratory
15. Fu C, Mielenz JR, Xiao X, Ge Y, Hamilton CY, Rodriguez M, Chen F, Foston M, Ragauskas A, Bouton J, Dixon RA, Wang Z (2011) Genetic manipulation of lignin reduces recalcitrance and improves ethanol production from switchgrass. *PNAS* 108(9):3803–3808
16. Murray I, Cowe I (2004) Sample preparation. In: Roberts CA, Workman J, Reeves JB (eds) *Near-infrared spectroscopy in agriculture*, vol 44. American Society of Agronomy, Inc., Crop Science Society of America, Inc., Soil Science Society of America, Inc., Madison, WI, pp 75–112
17. Vogel KP, Dien BS, Jung HG, Casler MD, Masterson SD, Mitchell RB (2011) Quantifying actual and theoretical ethanol yields for switchgrass strains using NIRS analyses. *Bioenergy Res* 4:96–110
18. Mixed hay: NIRS Forage and Feed Testing Consortium, June 2007 mixed hay calibration, file name: mh50-3. Parameters used: DM, CP, ADF, dNDF48, NDF, Ca, P, K, Mg, ash, fat, lignin, RUP
19. Lorenz AJ, Anex RP, Isci A, Coors JG, de Leon N, Weimer PJ (2009) Forage quality and composition measurements as predictors of ethanol yield from maize (*Zea mays* L.) stover. *Biotechnol Biofuels* 2(1):5
20. SAS 9.3 TS Level 1M2. SAS Institute, Cary
21. Arthur JC (1934) *Manual of rusts in United States and Canada*. Science Press, Lancaster
22. Jung HG, Vogel KP (1992) Lignification of switchgrass (*Panicum virgatum*) and big bluestem (*Andropogon gerardii*) plant parts during maturation and its effect on fibre degradability. *J Sci Food Agric* 59:169–176
23. Wilson JP, Gates RN, Hanna WW (1991) Effect of rust on yield and digestibility of pearl millet forage. *Phytopathology* 81(2):233–236
24. Queiroz OCM, Kim SC, Adesogan AT (2012) Effect of treatment with a mixture of bacteria and fibrolytic enzymes on the quality and safety of corn silage infested with different levels of rust. *J Dairy Sci* 95(9):5285–5291
25. Johnson JC, Gates RN, Newton GL, Wilson JP, Chandler LD, Utley PR (1997) Yield, composition, and in vitro digestibility of temperate and tropical corn hybrids grown as silage crops planted in summer. *J Dairy Sci* 80(3):550–557
26. Manners M (1982) Pathways of glucose assimilation in *Puccinia graminis*. *J Gen Microbiol* 128(11):2621–2630
27. Bartnicki-Garcia S (1968) Cell wall chemistry, morphogenesis, and taxonomy of fungi. *Annu Rev Microbiol* 22:87–108
28. Silva MC, Nicole M, Rijo L, Geiger JP, Rodrigues CJ (1999) Cytochemical aspects of the plant-rust fungus interface during the compatible interaction *Coffea arabica* (cv. Caturra)–*Hemileia vastarix* (race III). *Int J Plant Sci* 160(1):79–91
29. Hammerschmidt R (1984) Rapid deposition of lignin in potato tuber tissue as a response to non-pathogenic fungi on potato. *Physiol Plant Pathol* 24(1):33–42
30. Zhang SH, Yang Q, Ma RC (2007) *Erwinia carotovora* spp. *carotovora* infection induced “defense lignin” accumulation and lignin biosynthetic gene expression in Chinese cabbage (*Brassica rapa* L. spp. *pekinensis*). *J Integr Plant Biol* 49(7):993–1002
31. Liu XY, Jin JY, He P, Gao W, Li WJ (2007) Effect of potassium chloride on lignin metabolism and its relation to resistance of corn to stalk rot. *Sci Agric Sin* 40:2780–2787
32. Karkonen A, Koutaniemi S (2010) Lignin biosynthesis studies in plant tissue cultures. *J Integr Plant Biol* 52(2):176–185
33. Ride JP (1978) The role of cell wall alterations in resistance to fungi. *Ann Appl Biol* 89:302–306
34. Xu H, Heath MC (1998) Role of calcium in signal transduction during the hypersensitive response caused by basidiospore-derived infection of the cowpea rust fungus. *Plant Cell* 10(4):585–597
35. Liu G, Hou CY, Wang DM (2010) Calcium influx is required for the initiation of the hypersensitive response of *Triticum aestivum* to *Puccinia recondite* f.sp. *tritici*. *Physiol Mol Plant Pathol* 74(3–4):267–273
36. Chotineerant S, Wansuksri R, Piyachomkwan K, Chatakanonda P, Weerathawom P, Sriroth K (2010) Effect of calcium ions on ethanol production from molasses by *Saccharomyces cerevisiae*. *Sugar Technol* 12(2):120–124